

Atoms in double- δ -kicked periodic potentials: chaos with long-range correlations

P.H. Jones, M. Stocklin, G. Hur, and T. S. Monteiro

Department of Physics and Astronomy, University College London, Gower Street, London WC1E 6BT, U.K.

(Dated: November 9, 2018)

We report an experimental and theoretical study of the dynamics of cold atoms subjected to closely-spaced pairs of pulses in an optical lattice. The experiments show the interplay between fully coherent quantum dynamics and a novel momentum-diffusion regime: for all previously-studied δ -kicked systems, chaotic classical dynamics shows diffusion with short-time (2 or 3-kick) correlations; here, chaotic diffusion combines with new types of long-ranged ‘global’ correlations, between all kick-pairs, which control transport through trapping regions in phase-space. Analytical formulae are presented and, with quantum localization, are used to analyse the experiments.

PACS numbers: 32.80.Pj, 05.45.Mt, 05.60.-k

The ‘ δ -kicked particle’ (δ -KP) is one of the most studied experimental and theoretical paradigms of classical Hamiltonian chaos. A particle is kicked periodically by a sinusoidal potential $V(x, t) = -K \cos x \sum \delta(t - n)$. For sufficiently large K , the motion is fully chaotic and the energy grows diffusively. Of particular interest in recent years has been the theoretical [1, 2] and experimental [3] investigation of the suppression of the classical diffusive process in its quantum counterpart, the quantum δ -kicked particle (δ -QKP). This phenomenon is generally termed ‘Dynamical Localization’ (DL). For $K \gg 1$ the diffusive growth of the classical energy is no longer bounded by phase-space barriers (tori) so persists indefinitely: for an ensemble of classical particles, the energy $E = \langle \frac{P^2}{2} \rangle = \frac{1}{2}Dt \simeq \frac{K^2}{4}t$ for all t . The corresponding quantum energy grows only up to a timescale $t^* \sim D/\hbar^2$ [4] and saturates at a value $\langle P^2 \rangle_{t \rightarrow \infty} \sim Dt^*$. The Texas experiments showed that cesium atoms in periodically pulsed waves of light were an ideal test-bed for quantum chaos. A broad range of interesting physical regimes were subsequently investigated: controlled decoherence [5], quantum accelerator modes [6] and delocalization induced by non-periodic kicking [7].

The chaotic diffusion is however not entirely uncorrelated [8] and there are corrections which have now been experimentally observed [9] due to 2-kick and 3-kick correlations. For example, a 2-kick correction appears because the ensemble averaged value for the correlation between the impulse at the n -th kick and that experienced 2-kicks later, $C_2 = \langle V'(x_n)V'(x_{n+2}) \rangle$ is generally non-zero, see [8, 12]. In [10, 11] it was further shown that, if the pulses are unequally spaced, the 2-kick corrections yield a local (in momentum) correction to the diffusion. In that case, $2E(P_0, t) = D(P_0, t) t$: for unequal kick spacings, both the diffusion rate and hence the energy, depend non-trivially on time and the relative initial momentum, P_0 , between the atoms and the standing wave of light.

In this work we report the first experimental and theoretical study of the 2δ -kicked particle (2δ -KP): a cloud of cesium atoms is exposed to a periodic sequence of closely spaced *pairs* of kicks. At the outset, one might expect that the diffusive behaviour here could be analysed

within the framework used in [9, 10], of diffusion with correlations between short sequences of 2 or 3 kicks, whether local or otherwise. However this approach fails to explain the experimental results. Further investigation showed that chaotic diffusion in the 2δ -KP was rather different from that seen in previously studied kicked systems. For the 2δ -KP one finds new corrections, which appear in families correlating all kicks democratically. These corrections are individually very weak, but become numerous with time and accumulate to eventually dominate the diffusive process. Moreover, these ‘global’ correlations can be associated with specific physical phenomena, namely the escape from and through ‘trapping’ regions in phase-space. We have identified diffusive regimes associated with three types of correlation: one is an ordinary 1-kick correlation, C_1 , the other two are new and are families with ‘global’ terms. The experimental behaviour depends on which correlations dominate at the point when the quantum dynamics suppresses the diffusion.

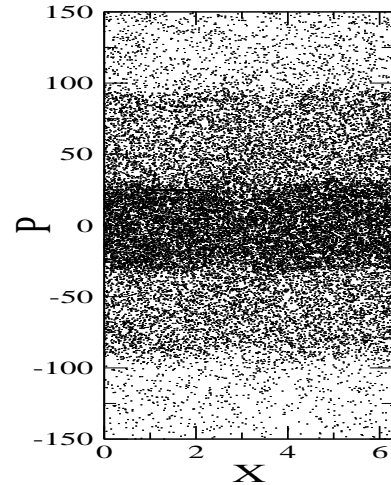


FIG. 1: Surface of Section diagram for an ensemble of particles, with $K = 7$ and $\epsilon = 0.1$, prepared with initial momentum $P_0 = 0$ at $t = 0$. The SOS illustrates the trapping of trajectories in phase space regions for which the momenta $p\epsilon \simeq \pm(2n + 1)\pi$.

The experimental apparatus is essentially like that de-

scribed in [11] and consists of a cloud of cesium atoms collected in a standard 6-beam MOT and cooled in an optical molasses to a temperature of $6\mu\text{K}$. The sinusoidal potential $V(x, t)$ is formed by two counter-propagating laser beams incident on the cloud with parallel polarisations. These are derived from a Titanium Sapphire laser, have an intensity of $4 \times 10^3 I_{\text{sat}}$ ($I_{\text{sat}} = 1.12 \text{mWcm}^{-2}$, the saturation intensity) in each beam and are detuned 2000Γ ($\Gamma = 2\pi \times 5.22 \text{MHz}$, the natural linewidth) below the D2 transition on cesium. The potential is switched on using acousto-optic modulators (AOMs) to create pulses as short as $t_p = 300 \text{ns}$, and each beam is controlled by a separate AOM so that a frequency difference Δf may be imposed upon the two beams and the potential moves with constant velocity in the laboratory frame. In this way we may explore the momentum dependence of the diffusion constant as in the rest frame of the potential the atomic momentum distribution has a non-zero mean value $P_0 \propto \Delta f$.

We now have two periods: τ , which represents a (long) timescale between the pairs of kicks, and ϵ , which represents a much smaller time interval between kicks in each pair. In the experiment, $\tau = 9.47 \mu\text{s}$, while five different separations of the closely-spaced pair, in the range $0.44 \mu\text{s}$ to $1.48 \mu\text{s}$ were used: $\epsilon = 0.047, 0.063, 0.094, 0.125$ and 0.156 . For these parameters and with the intensity and detuning as above, we have an effective value of $\hbar = 1$ while the kick-strength, $K = 3.3$ ($\pm 10\%$ due mainly to the uncertainty in measuring the intensity in the laser beams). Up to 100 kicks were applied before the cloud of atoms was allowed to evolve freely in the dark for 15ms. A pair of near-resonant imaging beams were then switched on and the fluorescence imaged on a CCD camera. From the spatial distribution of the fluorescence the momentum distribution was extracted and $\langle P^2 \rangle$ calculated.

The corresponding classical behaviour of the 2δ -KP would be given by evolving a 2-kick map:

$$\begin{aligned} p_i &= p_{i-1} + K \sin x_{i-1} \\ x_i &= x_{i-1} + p_i \epsilon \\ p_{i+1} &= p_i + K \sin x_i \\ x_{i+1} &= x_i + p_{i+1} \tau \end{aligned}$$

It is instructive to begin by considering the classical evolution of an ensemble of particles all initially at time $t = 0$, with momentum $p = P_0$ for which $P_0 \epsilon = (2n + 1)\pi$ and $n = 0, 1, \dots$. These particles experience a kick $K \sin x_{i-1}$ followed by another at $\simeq K \sin(x_{i-1} + \pi)$ which in effect cancels the first. Conversely in the case $P_0 \epsilon = 2n\pi$ a series of near-identical kicks produces initially rapid energy growth. Other P_0 produce intermediate behaviour. This behaviour follows from the unsurprising fact that the presence of the short time interval, ϵ , results in a non-zero kick-to-kick correlation C_1 . In contrast, for the Standard Map and *all* other previously studied atomic δ -kicked systems, $C_1 = 0$.

We show, in Fig.1, Surface of Section plots obtained from an ensemble initially with $P_0 = 0$, but randomly distributed in position x , for $K = 7$, $\epsilon = 0.1$. It is clear that, though the phase-space here is fully chaotic, trajectories ‘stick’ at the values of $p\epsilon \simeq \pm(2n + 1)\pi$. By calculating C_1 explicitly, after N pairs of kicks, one can begin a more precise analysis:

$$C_1(N, P_0) = K^2 \cos P_0 \epsilon [J_0(K\epsilon) - J_2(K\epsilon)] \sum_{j=1}^N (J_0(K\epsilon))^{2j-2} \quad (0.1)$$

Physical time is $t = N(\tau + \epsilon)$. We can re-scale variables so $\tau = 1$ and $t \simeq N$. The ensemble-averaged energy E of the atom cloud at time t , corrected by Eq.0.1 would be given by $2E = \langle (P_t - P_0)^2 \rangle \simeq K^2 T / 2 + C_1(t, P_0)$ (where $T = 2N = 2t$). It is easily shown that for short times C_1 grows linearly in time, while for longer times it saturates to a constant value, after a time $t_1 \sim \frac{10}{(K\epsilon)^2}$. On this time-scale, the kick-to-kick contributions decay to zero. Since C_1 is a single correlation term, analogous to those studied in [10] we have here been able to simply extend the usual analysis of [10, 12]. For small $K\epsilon$, $J_2(K\epsilon) \simeq 0$, so for short times ($t \ll t_1$) we can write for the energy, $2E = \langle (P_t - P_0)^2 \rangle \simeq K^2 T / 2 [1 + \cos P_0 \epsilon]$. The validity of this formula for $t \ll t_1$ is seen in the experimental data in Fig.2(a).

Fig.2 show the energy absorbed by the cesium atoms, as a function of P_0 . Three separate values of ϵ were considered. For each ϵ , the energy was measured, after 100 kicks (but here $t^* \sim 40$) for many values of P_0 . In every case, at time $t = 0$, the atom cloud had energy $\langle (P_{t=0} - P_0)^2 \rangle \simeq 30$, indicated by the horizontal dot-dashed line.

The experimental data of Fig.2(a) is the most straightforward to understand: here, $t_1 \sim 450$, so $t^* \ll t_1$ so the energy absorption was arrested in the regime $t \ll t_1$. An ensemble of classical particles, initially at momenta $P_0 \epsilon \simeq \pm(2n + 1)\pi$, absorbs no energy while for $P_0 \epsilon \simeq \pm 2n\pi$, energy absorption is maximal.

Fig.2(c), on the other hand, was the most surprising. It corresponds to a regime $t^* > t_1$. It shows a clear reversal of the behaviour seen in Fig.2(a): atoms initially prepared at or near the momentum-trapping regions end up with more energy than those prepared in the enhanced momentum diffusion regions. In fact, atoms which are prepared furthest from the momentum trapping regions, absorb the least energy.

This counter-intuitive observation motivated a more careful look at the mathematical model of the diffusive process of the 2δ -KP. This exposed a collection of terms involving averaging products of the form $\sin x_i \sin x_\mu$, where $\mu < i$ but is otherwise arbitrary; while i represents any of the *second* kicks in the pair. For each μ we obtain a correction of the form $4K^2 \cos P_0 \epsilon J_1^2(K\epsilon) \sum_j (J_0(K\epsilon))^{2j-3}$. These terms are negligibly small ($O(K\epsilon)^2$ relative to C_1). However since

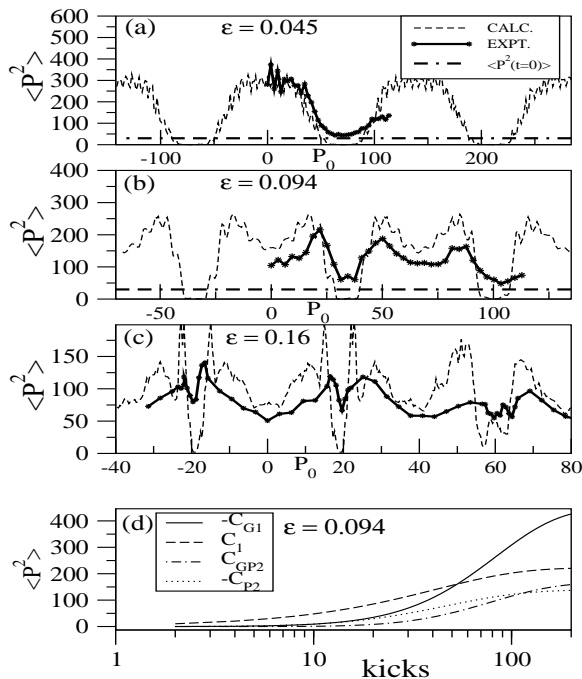


FIG. 2: Experimental results for 2δ -KP realisation with cesium atoms. Each data point (star) shows the energy absorbed (after 100 kicks, $K = 3.3$, $\hbar = 1$) by a cloud of atoms with average momentum $p = P_0$ (relative to the optical lattice) at initial time, $t = 0$. With increasing ϵ , we see the minima (maxima) in the energy flip into maxima (minima) as the ‘global’ correlation family C_{G1} gradually overtakes the nearest-neighbour correlation C_1 . The dashed lines represent a classical simulation using 100,000 particles all with momenta $= P_0$ at $t = 0$, and K within the range $3.3 \pm 10\%$. (a) $t^* \ll t_1 \simeq 1/(K\epsilon)^2$. Regime dominated by the one-kick correlation C_1 . Atoms prepared near the trapping regions ($P_0\epsilon \sim (2n+1)\pi$) remain trapped. Results follow closely the formula $\langle P^2 \rangle \simeq K^2 T/2(1 + \cos P_0\epsilon)$. (b) $t^* \sim 1/(K\epsilon)^2$. Regime for which C_1 competes with the ‘global’ correlation family C_{G1} . This begins to expose the inverted peaks of the Poisson correlation terms C_P , which determine the trapping very close to the resonant condition ($P_0\epsilon = (2n+1)\pi$). (c) $t^* > 1/(K\epsilon)^2$. Regime dominated by C_{G1} , but sharp inverted peaks due to C_P are still visible. (d) Competition between C_1 , C_{G1} and leading order Poisson terms. At short times, the global correlations are negligible, but at later times, the accumulation of (individually weak) global correlations overtake the corresponding C_1 and C_{Pm} terms: when the global terms become dominant, all the atoms have escaped from the trapping regions.

we sum over all $\mu < i$ their numbers accumulate with time and the net contribution of this ‘global’ correlation family is:

$$-C_{G1}(N, P_0) = 4K^2 \cos P_0\epsilon J_1^2(K\epsilon) \sum_{j=1}^N (j-1)(J_0(K\epsilon))^{2j-3}. \quad (0.2)$$

It is easily shown that, though negligible at short times,

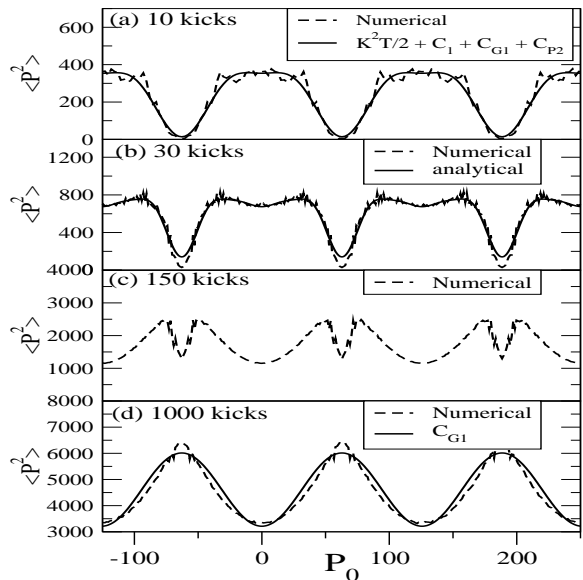


FIG. 3: The figure plots the energy absorbed by an ensemble of 100,000 classical particles, all with $p = P_0$ at $t = 0$, as a function of initial momentum (dashed line). These numerics are superposed with analytical formulae obtained for the diffusion (solid line). $K = 7$ and $\epsilon = 0.05$ in every figure, but the number of kicks, $2N$, varies. Note the behaviour in the trapping region $P_0 \simeq \pi/\epsilon \simeq 60$: the energy absorbed is a minimum at short times but turns into a maximum at long times. (a) Results at short time (10 kicks), dominated by the one-kick correlation C_1 . (b) Results at a time for which C_1 competes with the ‘global’ de-phasing family C_{G1} . This exposes the ‘Poisson-sum-formula’ corrections: a family of corrections of the form $C_{Pm} \propto \cos mP_0\epsilon$, ($m \geq 2$) combine to give a series of inverted peaks in the trapping regions (c) All three corrections C_P , C_1 and C_{G1} compete (d) At $t > 500$ the longest lived correction, C_{G1} dominates. The Poisson corrections have changed sign: the inverted peaks of (c) (indicating trapping), have ‘flipped over’ to give a series of positive peaks which give the maxima a ‘pointed’ appearance. The counter-intuitive result, that particles initially prepared in the momentum-trapping regions will be the ones which will acquire the most energy, is evident.

this term grows quadratically at small t and eventually overtakes C_1 . It has opposite sign to C_1 ; we interpret it as a term which reflects the gradual de-phasing of the resonant effects of C_1 -such as the kick-cancellation/trapping regions with $P_0\epsilon \sim (2n+1)\pi$. At long times the behaviour is dominated by C_{G1} and hence we see that the energy absorption is *maximal* for particles prepared near $P_0\epsilon \simeq \pm(2n+1)\pi$.

Fig.2(b) corresponds to a particularly interesting regime, where $C_1 \sim C_{G1}$. The $\cos P_0\epsilon$ correction is partly cancelled, exposing a series of narrow dips in the energy. The origin of these dips is in a series of terms $C_{Pm} \propto \cos mP_0\epsilon$. When summed these produce behaviour reminiscent of the Poisson sum formula $\sum_m (-1)^m \cos mP_0\epsilon = \sum_n \delta(P_0\epsilon - (2n+1)\pi)$. The amplitudes of the C_{Pm} terms vary with time and only a finite

number of harmonics ($m < 10$ typically) contributes at any given time. Hence we get a series of broadened peaks. Nevertheless, for this reason, we term these corrections the Poisson term, $C_P = \sum C_{P_m}$ and where:

$$C_{P_m}(N, P_0) \propto K^2 \cos mP_0 \epsilon F_m(t) \prod_{n=1}^{m-1} J_1^2(nK\epsilon). \quad (0.3)$$

$F_m(t)$ is a time function which grows as $\sim t^m$. Though these terms are small ($O(K\epsilon)^{2m-2}$) they will contribute when $t^m(K\epsilon)^{2m-2} \sim 1$. Each of these terms also has a partner ‘global’ family of opposite sign, C_{GP_m} ($O(K\epsilon)^{2m}$), which increase as $\sim t^{m+1}$. Fig.2 (d) shows the behaviour of the $m = 2$ Poisson terms in comparison to C_1 and C_{G1} . As m increases terms become less significant and for each m the global correlation always dominates C_{P_m} at long times. There are additional, even higher-order, $\cos nP_0 \epsilon$ terms ($n \geq 1$) of similar form to C_{P_m} and C_{GP_m} above and a group of terms involving products of the form $\sin^2 x_i$ which may contribute, particularly to C_{P_2} .

In Fig.3 we compare numerical (classical) calculations at $K = 7$, $\epsilon = 0.05$, with the behaviour predicted by the correlations. In Fig.3(a) we look at short times and see that we can accurately match the energy absorption by including only the three lowest order diffusive corrections, ie those which increase linearly or quadratically in time (C_1 , C_{G1} , C_{P_2}). At later times ($t < 50$ or so), we obtain good agreement by including all the above terms up to order J_1^{10} and $m = 4$: the inverted peaks corresponding to the trapping regions are quite well reproduced, as seen in Fig.3(b). At extremely long times, we can obtain good results simply from the leading global family C_{G1} . We also clearly see, in Fig.3(d), the inversion of the behaviour seen at earlier times: atoms prepared within the trapping regions give positive peaks, since C_{GP_m} dominates. The $0 - th$ order term is $\langle P^2 \rangle \simeq K^2 T/2$ at very short times, then gradually slows down to an asymptotic value $\simeq K^2 T/16$ (obtained numerically) at long times. The analytical curves in Fig.3 are shifted vertically by a constant amount.

In conclusion, we have presented and analysed an experimental realisation of a $2\delta - KP$ and shown that it corresponds to a type of diffusion quite different from the Standard Map. This is a rich and complex system and many questions remain open. On the classical side,

certain aspects of the interactions and lifetimes of the different types of correlations are not yet well understood. Although we have a generic handle on this system with the diffusion correlations, further insight might be gained by detailed knowledge of classical trajectories. For lower values of $K\epsilon$, a thin band of islands and eventually unbroken tori appears first around $p\epsilon \simeq \pm(2n+1)\pi$. At this point, clearly, there will be no escape through the trapping regions and beyond the very shortest times ($t_1 \ll 1/(K\epsilon)^2$) the diffusive correlation approach would fail everywhere. We expect regions permeated by broken phase-space barriers to persist at the parameters such as eg. Fig.1 and to account for the trapping regions.

The quantum behaviour is also not fully understood. Though clearly some key features can be modelled qualitatively in Fig.2 by adjusting the number of kicks and K (by up to 10% in the classical numerics of Fig.2), the quantum dynamics will involve tunnelling and dynamical localization (DL) effects which can introduce substantial differences with the classical behaviour. Further investigation of the DL in this system is necessary: its Floquet states are localised, like in the standard $\delta - KP$. But in the latter, localization lengths, L , are quite uniform with exponential localization and $L \sim \frac{D}{\hbar}$, while in the $2\delta - KP$, values of L can vary by about 3 orders of magnitudes for the parameters considered here [14].

Although the $t \ll t_1$ experimental regime (seen in Figs. 2(a) and 3(a)) is in some sense the least surprising in terms of the diffusive process, it is worth noting its potential for atomic manipulation. Interest in the 2δ -KP experiment was initially stimulated by its potential applications in manipulating atoms in devices like an atom ‘chip’ [13]. In [10] it was proposed that a local diffusion rate $D(P_0)$, could be exploited for ‘filtering’ cold atoms according to their velocity. For selected P_0 the atoms could pass the device unperturbed, while other momenta would absorb a substantial amount of energy and would be dispersed. The 2δ -QKP showed a far stronger experimental signature than the system in [10, 11] which relied on a two-kick, C_2 , correlation (note that $C_2 \neq C_{P_2}$). A much stronger velocity-selective effect, due to the C_1 , correlation is seen for the 2δ -QKP. The inverted peaks of the C_p correlations could also be used to select a narrow band of velocities with $P_0 \simeq \pi/\epsilon$.

The authors thank Thibaut Jonckheere for helpful discussions. This work was supported by the EPSRC.

-
- [1] G. Casati, B.V. Chirikov, Izraelev F.M., and J. Ford in "Lecture notes in Physics", Springer, Berlin **93**, 334 (1979).
- [2] S. Fishman, D.R. Grempel, R.E. Prange, Phys. Rev. Lett. **49**, 509 (1982).
- [3] F. L. Moore, J. C. Robinson, C. F. Bharucha, Bala Sundaram, and M.G. Raizen Phys. Rev. Lett. **75**, 4598 (1995).
- [4] D. L. Shepelyansky Phys. Rev. Lett. **56**, 677 (1986)
- [5] B.G. Klappauf, W.H. Oskay, D.A. Steck, and M.G.Raizen, Phys. Rev. Lett. **81**, 1203 (1998).
- [6] M.B.d’Arcy,R.M. Godun, M.K. Oberthaler,D. Cassettari, and G.S. Summy, Phys. Rev. Lett. **87**, 74102 (2001).
- [7] P. Szriftgiser, J. Ringot, D. Delande, and J-C Garreau Phys. Rev. Lett.**89**, 224101 (2002)
- [8] A.J. Lichtenberg and M.A. Lieberman, 'Regular and Chaotic Dynamics', Springer-Verlag, New York (1992).
- [9] B.G. Klappauf, W.H. Oskay, D.A. Steck, and

- M.G.Raizen, Phys. Rev. Lett. **81**, 4044 (1998).
- [10] T. Jonckheere, M. R. Isherwood and T. S. Monteiro, Phys. Rev. Lett. **91**, 253003 (2003).
- [11] P.H.Jones, M.Goonasekera, H.E. Saunders-Singer and D.Meacher *quant-physics/0309149*.
- [12] A. B. Rechester and R. B. White, Phys. Rev. Lett. **44**, 1586 (1980).
- [13] E.Hinds and I.G.Hughes, 'Magnetic atom optics: mirrors, guides traps, and chips for atoms' (Review article) J. Phys. D. **32**, 119 (1999).
- [14] G. Hur et al, in preparation.